

MAGNETIC RESONANCE IMAGING OF WATER CONCENTRATION IN LOW MOISTURE CONTENT WOOD

M. Bryce MacMillan

Research Associate
Department of Physics, Faculty of Science

Marc H. Schneider†

Professor
Wood Science and Technology
Faculty of Forestry and Environmental Management

Allan R. Sharp

Professor and Dean of Science
MRI Centre, Department of Physics

and

Bruce J. Balcom

Professor and Director
MRI Centre, Department of Physics
University of New Brunswick
P.O. Box 4400
Fredericton, N.B.
Canada E3B 5A3

(Received February 2001)

ABSTRACT

A new magnetic resonance imaging (MRI) technique, termed SPRITE (Single Point Ramped Imaging with T_1 Enhancement) permits visualization of water content in previously inaccessible wood fiber systems. We demonstrate the superiority of SPRITE methods, in comparison to conventional MRI methods, for studying fluid content in low water content wood materials. SPRITE and conventional MRI images were acquired from four species of wood, equilibrated at multiple moisture content levels. Both methods were also used to examine relative moisture content during forced drying of a white ash wood sample.

Keywords: Imaging, MRI, magnetic resonance, SPRITE, wood, water, hydration, moisture, drying.

INTRODUCTION

Wood has water content, post-harvest, which is usually much greater than required for the finished wood product. Therefore drying is required during processing. Some wood products are impregnated with fluids during processing. After drying below the fiber saturation point (about 30% moisture content), wood is porous and strongly hygroscopic. It

gains and loses moisture as atmospheric conditions change. Fluid (principally water) distribution and flow in wood materials are thus of great practical interest and have been extensively studied (Skaar 1988). All currently used methods for determining water content within intact wood materials measure either the whole sample, or a single position in the sample, at one time. A practical method for measuring water concentration in wood materials, spatially and temporally resolved, does

† Member of SWST.

not yet exist. A noninvasive technique capable of such measurements would greatly facilitate water distribution and transport studies in wood. At least in principle, magnetic resonance imaging (MRI) is ideally suited to this task.

MRI has evolved into a powerful analytical tool in both medical and material sciences (Blümich 2000; Callaghan 1991). However, despite a widespread and ever-growing range of applications, MRI has not been extensively exploited in wood science. In part this is due to the inherent limitations of conventional (spin-echo) MRI methods. Slice selective spin-echo imaging requires a sample spin-spin relaxation time, T_2 , which is longer than approximately 10 ms. Analogous non-slice selective measurements require T_2 relaxation times of at least 1 ms. In our experience, low water content wood fiber materials present spin-spin relaxation times (signal lifetimes) of well under 1 ms, and thus cannot be reliably observed and quantified with spin-echo MRI methods.

Free water, with a relatively long signal lifetime (T_2), is relatively easy to image using MRI. It has been demonstrated, with varying degrees of success, that conventional MRI can visualize the internal structure of wood (Wang and Chang 1986; Hall et al. 1986a, 1986b; Chang et al. 1989; Filbotte et al. 1990; Coates et al. 1998), distinguish between healthy tissue and rot (Filbotte et al. 1990; Pearce et al. 1997a, 1997b), characterize water in the different internal environments (Araujo et al. 1992; Menon et al. 1989), track the absorption of preservatives (Meder et al. 1999), and map moisture content during drying (Hall and Rajanayagam 1986; Quick et al. 1990).

Bound water, with hindered local motion, has 'solid-like' magnetic resonance characteristics, most notably a short observable signal lifetime, T_2 . The short T_2 of solid-like materials means that bound water will be largely invisible with spin-echo MRI methods. This has the unfortunate consequence that wood in which the moisture content is low cannot be investigated with conventional MRI. In the

most comprehensive MRI examination of wood drying in the literature, Araujo et al. (1992) used a 17% moisture content as a lower limit for conventional MRI examination. Many end-use wood applications require significantly lower moisture contents. In kiln-drying hardwood lumber, the usual target MC is 6%. The MC in wood building materials can be as low as 4% inside the heated space, and 10 to 12% in the structure. Particles and flakes for oriented strandboard are typically dried to the 3 to 4% range before gluing.

Work in our laboratories, and in that of other investigators (Riggin et al. 1979; MacGregor et al. 1983; Peemoeller et al. 1985; Waana 1994), has shown that it is possible, in bulk magnetic resonance measurements, to detect the magnetic resonance (MR) signals from bound water. Our current study was triggered by a very simple question: Can these short-lived signals be spatially encoded to form a useful MRI image?

Single Point Ramped Imaging with T_1 Enhancement (SPRITE) imaging techniques (Balcom et al. 1996; Balcom 1998), make it possible to image solid-like systems in which the MR signals are short-lived. SPRITE experiments require only that the apparent spin-spin relaxation time of the sample, denoted T_2^* and closely related to T_2 , be on the order of 10 μ s or more. This is more than an order of magnitude shorter than is possible with conventional MRI methods! In this work, we demonstrate the utility of SPRITE for visualization of low moisture content wood materials. SPRITE and spin-echo images were acquired from four species of wood equilibrated at multiple moisture content levels. In addition, both methods were used to acquire images of wood undergoing active drying.

CONVENTIONAL MI AND SPRITE

Conventional two-dimensional spin-echo imaging typically employs frequency encoding in one spatial direction, and phase encoding in an orthogonal direction (Fig. 1). Frequency encoding requires dephasing and re-

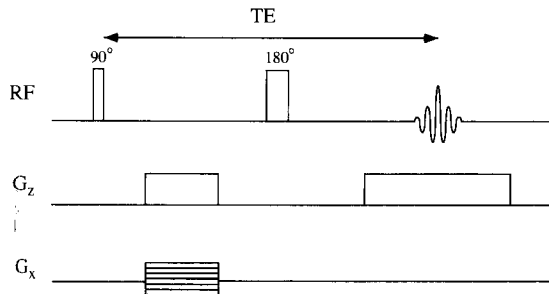


FIG. 1. Timing diagram of the conventional spin-echo method in two dimensions. Frequency encoding is employed along the primary direction, z , phase encoding along the secondary axis, x . Signal is averaged over the y dimension. A spin echo forms at time TE after the first radio frequency (RF) pulse. G_z and G_x denote the gradients along the z and x directions.

focusing magnetic field gradients (G_z), as well as two radio frequency (RF) pulses (90° and 180°) which produce a spin-echo at a time TE after the initial RF pulse. A signal is acquired in the presence of the refocusing magnetic field gradient, and numerous data points, typically 64, are collected during echo formation and decay. Phase encoding involves incrementing the phase of the MR signal (for each echo) in discrete steps, also typically 64, with an orthogonal phase encoding magnetic field gradient (G_x). The experimental image is reconstructed from the frequency and phase encoded data set through a two-dimensional Fourier transform (Blümich 2000; Callaghan 1991).

The echo intensity decays by a factor of e^{-TE/T_2} so that in samples where $T_2 \ll TE$, spin-echoes are virtually undetectable, and image formation impossible. The minimum echo time is determined by the experimental conditions. This minimum time is a function of the RF pulse lengths (which are long for slice selective experiments), the duration and switching times of the magnetic field gradients, and the time required to acquire the experimental data points.

Single point imaging (SPI) methods are generically better suited to imaging solid-like systems. SPI methods are pure phase encode techniques in which a single point on the sig-

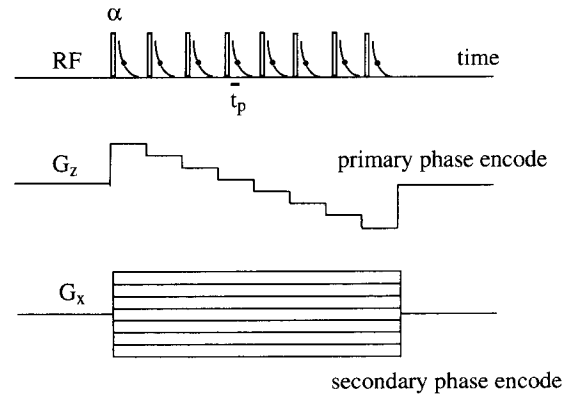


FIG. 2. Timing diagram of the SPRITE method in two dimensions. The phase encode gradient (G_z) is ramped along the primary direction, z . The secondary direction, x , employs a stepped phase encode gradient (G_x). Signal is averaged over the y dimension. A single complex point is acquired at each gradient step a time t_p after the application of a radio frequency (RF) pulse, with flip angle α .

nal resulting from the RF excitation is sampled in a fixed encoding time t_p after the RF pulse (Axelson et al. 1995). Unlike frequency encoded images, SPI images are free from distortions due to inhomogeneities in the static magnetic field, B_0 , magnetic susceptibility variations, and chemical shift (Gravina and Cory 1994). In addition, SPI methods avoid the line width restriction on resolution inherent to frequency encoding methods (Gravina and Cory 1994). Resolution and sensitivity in SPI methods are principally determined by maximum gradient strength and the chosen t_p .

The basic SPI technique is not a widely used technique because of the extensive gradient switching required and lengthy data acquisition times. A recently developed SPI variant, SPRITE (Single Point Ramped Imaging with T_1 Enhancement) successfully overcomes these limitations. In the SPRITE method (Balcom et al. 1996), the primary phase encode gradient (G_z) is ramped in discrete steps and an RF pulse applied at each step with a single data point collected following each pulse (Fig. 2). The use of the ramped phase gradient results in shorter acquisition times and minimal gradient vibration. The SPRITE technique has proven applicable to a wide range of material

science systems (Balcom 1998) including studies of the gas phase (Prado et al. 1999), food materials (Troutman et al. 2001), polymers (Kennedy et al. 1998), and concrete materials (Beyea et al. 1998). The MR characteristics of the bound water in wood materials are remarkably similar to the MR properties observed in low water content food materials (Troutman et al. 2001) and in the solid bone mineral phase (Balcom 1998).

Experimental

For the static experiments, images were obtained from samples of white ash (*Fraxinus americana*), beech (*Fagus grandifolia*), yellow birch (*Betula alleghaniensis*), and red pine (*Pinus resinosa*). Samples measuring approximately 2.5 cm × 2.0 cm × 4.5 cm in the radial, tangential, and longitudinal directions, respectively, were equilibrated at relative humidities of 50, 40, 30, and 15%. These humidities correspond to moisture contents (MC) of 8.5, 7.7, 6.7, and 4.1% for the beech samples. The moisture content was calculated on the basis of the dry wood mass. The dry mass was obtained after all other experiments had been completed by heating the samples at 110°C for two weeks.

For all but the lowest MC, hydration equilibrium was achieved in a Caron 6010 (Caron, Marietta, OH) controlled humidity chamber. Relative humidities of 50, 40, and 30% were used, at a temperature of 30°C. For the 4.1% MC, the sample was equilibrated at room temperature in a desiccator jar over a saturated solution of LiCl·H₂O. This maintains a relative humidity of 15% at 20°C (CRC Handbook 2000). Samples were kept in these environments until no further change in mass was measured. The sample handling time from chamber to magnet was several minutes.

SPRITE MRI measurements were performed at ambient temperature with a Tecmag (Tecmag, Houston, TX) Libra S-16 console in a Nalorac (Nalorac Cryogenics Inc, Martinez, CA) 2.4 Tesla, 32-cm inside diameter (i.d.) horizontal bore superconducting magnet. A

Nalorac, water-cooled, 7.5 cm i.d. gradient set (maximum gradient strength 100 G/cm) powered by Techron (Techron, Elkhart, IN) 8710 amplifiers was used. The RF probe was a 47 mm i.d. (Morris Instruments, Ottawa, ON) eight-rung quadrature birdcage probe, driven by a 2 kW AMT (AMT, Brea, CA) 3445 RF amplifier.

A rubber standard was present in each experiment to normalize the image data. The image intensity was scaled, where required, to maintain the intensity of the rubber reference constant. The minimal scaling required corrected for small variations in the day to day instrument sensitivity over the course of these experiments.

SPRITE moisture content experiments were performed at 99.3 MHz using a phase encoding time, t_p , of 50 μ s, a recovery time, TR, of 2 ms, an RF flip angle, α , of 8°, and a delay between successive gradient ramps of 300 ms. The field of view was 8 cm × 8 cm, and 64 scans were acquired per image, requiring approximately 30 min. The nominal image resolution, 64 × 64 pixels, was 1.3 mm.

Spin-echo moisture content measurements were performed at ambient temperature with a General Electric (GE NMR Instruments, Fremont, CA) CSI II spectrometer in an Oxford (Oxford Instruments, Oxford, England) 2.0 Tesla, 31 cm i.d. horizontal bore superconducting magnet. A General Electric Acustar 15 cm i.d. gradient set (maximum gradient strength 10 G/cm), powered by Techron 8608 amplifiers, was employed. The RF probe was a home-built, single channel, 57 mm i.d., 48 rung birdcage. The GE spectrometer had a built-in 100 watt amplifier. A rubber standard was present in each experiment to normalize the image data as previously described.

Spin-echo moisture content experiments were performed at 85.6 MHz with an echo time, TE, of 1100 μ s, a repetition time, TR, of 100 ms, and a dwell time of 5 μ s. The 90° pulse width was 29 μ s, the field of view was 9 cm × 9 cm, and 256 scans were acquired per image. The image, 64 × 64 pixels, had a

nominal resolution of 1.4 mm with a total scan time of approximately 55 min.

In the active drying experiments, a sample of white ash measuring approximately 2.5 cm × 2.0 cm × 4.5 cm in the radial, tangential, and longitudinal directions, respectively, was saturated with water (moisture content 108%) using vacuum infusion. A heated air stream was used for drying. As this was a qualitative experiment, air temperature and flow rate were not monitored. Spin-echo and SPRITE images were acquired every 45 min for 23 h during drying, with the sample remaining in the MRI magnet. The final moisture content was determined to be 1.5%. Spin-echo and SPRITE images of the active drying process were both undertaken on the Tecmag instrument in the 2.4 Tesla magnet.

SPRITE active drying experiments were performed at 99.3 MHz using a phase encoding time, t_p , of 50 μ s, a recovery time, TR, of 2 ms, an RF flip angle, α , of 11°, and a delay between successive gradient ramps of 300 ms. The field of view was 8 cm × 8 cm, and 16 scans were acquired per image, requiring approximately 8 min. The imaging time was shortened to minimize effects from drying during the acquisition. The nominal image resolution, 64 × 64 pixels, was 1.3 mm.

Spin-echo active drying experiments were performed at 99.3 MHz with an echo time, TE, of 1200 μ s, a repetition time, TR, of 300 ms, and a dwell time of 15 μ s. The 90° pulse width was 12.6 μ s, the field of view 8 cm × 8 cm, and 16 scans were acquired per image. The nominal image resolution, 64 × 64 pixels, was 1.4 mm, for a total scan time of approximately 5 min.

RESULTS AND DISCUSSION

Two-dimensional spin-echo and SPRITE images, averaged over the radial direction, of a beech sample hydrated to 8.5, 7.7, 6.7, and 4.1% moisture contents are presented in Fig. 3. These moisture contents correspond to absolute water masses of 1.2, 1.1, 1.0, and 0.6 g, respectively. In these images, the sample's

tangential direction was parallel to the magnetic field B_0 . The images show the tangential plane of the wood. The image field of view in the SPRITE images is somewhat smaller than in the spin-echo images. The small square apparent in each image is a rubber reference sample. In the third spin-echo image, the rubber reference was positioned on the opposite side of the sample. This has no effect on the image analysis. The spot in the lower left quadrant of the spin-echo images is background signal from the RF probe.

One reasonably anticipates that the image intensity will decrease with reduced MC, as is observed in Fig. 3. This is the result of several factors. The signal intensity will be lower as a direct result of the lower water concentration. More subtly, the remaining water will have shorter spin-spin relaxation times. In analogous soft porous materials, as free water is removed, not only does the relative proportion of bound water increase, but channels and pores within the material constrict, restricting the mobility of the remaining water (MacMillan 1996; Klafter and Drake 1989). The residual water appears more solid-like and has shorter spin-spin relaxation times. The effect on image intensity, of a reduction in the overall water T_2 (or T_2^*), depends on the imaging method and acquisition parameters employed.

In the spin-echo method, if a sufficient recovery time is allowed between successive echoes, as was the case here, the signal intensity, S , is given by:

$$S = \rho_0 e^{-TE/T_2} (1 - e^{-TR/T_1}) \approx \rho_0 e^{-TE/T_2} \quad (1)$$

where ρ_0 is the proton (water) density and T_2 is the spin-spin relaxation time. In our measurements, TE s of 1100 μ s and 1200 μ s were employed.

Bulk MR measurements of these wood materials show that the T_2 relaxation behavior is complex, and not surprisingly the relaxation times are multi-exponential (Araujo et al. 1992). We measure at least two different relaxation times in each sample. The long one, many milliseconds long, is attributed to relatively mobile water molecules. The shorter

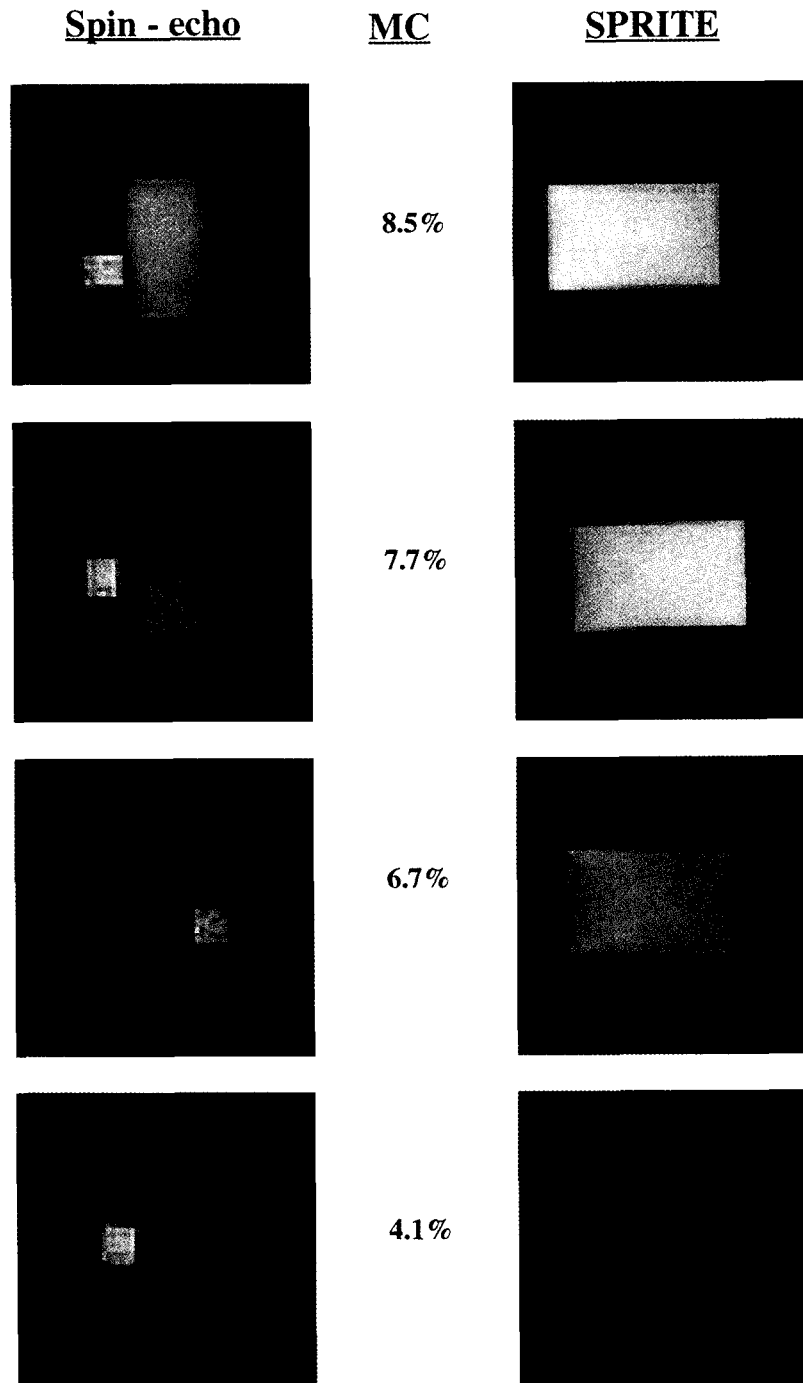


FIG. 3. Spin-echo and SPRITE images of a beech sample equilibrated to 8.5, 7.7, 6.7, and 4.1% moisture contents. The field of view is 9 cm \times 9 cm in the spin-echo images, and 8 cm \times 8 cm in the SPRITE images. The images are scaled to keep the reference intensity constant within each series of spin-echo or SPRITE images. Note that the image intensity from the wood specimen in the final spin-echo image has virtually disappeared.

one, a few hundred microseconds long, arises from bound water and possibly other ^1H containing components in the wood. As a result, when free water is removed from the wood, the signal rapidly disappears as T_2 decreases. The spin-echo image intensity in Fig. 3 thus decreases due to a decrease in the value of both the first *and* second terms on the right of Eq. (1).

In SPI and SPRITE experiments, the signal amplitude in the longitudinal steady state, S , following an RF pulse of flip angle α , is given by (Balcom et al. 1996):

$$s = \rho_0 e^{-t_p/T_2^*} \left(\frac{1 - e^{-TR/T_1}}{1 - \cos(\alpha)e^{-TR/T_1}} \right) \sin(\alpha) \quad (2)$$

where ρ_0 is the proton (water) density, t_p is the phase encode time, T_2^* is the apparent spin-spin relaxation time, T_1 is the spin-lattice relaxation time, and TR is the repetition time between successive pulses. Bulk measurements revealed that the T_1 relaxation time was also multi-exponential, with a short component of several milliseconds and longer ones on the order of tens of milliseconds. Both the spin-echo and SPRITE imaging experiments minimized T_1 effects on the observed image intensity through an appropriate choice of acquisition parameters.

Bulk MR measurements reveal at least two T_2^* components in each wood sample, the longest of which is on the order of 1 ms, with the shorter component several hundred microseconds. In our imaging experiments, we used an encoding time, t_p , of 50 μs , and the RF pulse flip angle α was intentionally kept small. This ensures that even the shortest T_2^* components are detected and that signal attenuation due to spin-spin relaxation was minimal. Under these conditions, Eq. (2) reduces to

$$S = \rho_0 \sin(\alpha) \quad (3)$$

The RF flip angle α is a chosen constant; therefore the SPRITE images are effectively maps of proton density, i.e., water concentration.

Both the spin-echo and SPRITE techniques gave satisfactory images at the higher mois-

ture contents. At lower MCs, however, signal loss degrades the image quality. This effect was very pronounced in the conventional spin-echo image. At the 4.1% level, the intensity and image quality are very poor. The effectiveness of the SPRITE technique is demonstrated most dramatically in the companion images from the lower levels of hydration, (Fig. 3). While the image intensity has decreased as a result of the water loss, the overall image quality remains high.

Although tempting, it is misleading to directly compare wood intensity/reference intensity for the two methods at fixed MC. The relaxation behaviors of the rubber and wood are different, and it is therefore expected that the two imaging methods will give different image intensities for the rubber standard. This is observed experimentally in Fig. 3. It is also anticipated that the signal to noise ratio will be different for the two sequences. A more meaningful comparison of the techniques will be an examination of how the wood intensity/reference intensity decreases as the wood MC decreases.

The standardized image intensities $S_{\text{wood/reference}}$ vs. MC from the spin-echo and SPRITE images for each wood species are presented in Figs. 4 and 5, respectively. These were obtained from each image by selecting a representative region from the wood and rubber, averaging the pixel intensities within these regions, then taking the quotient of the two intensities. At the various moisture contents, the same region in each sample was selected. The variability within each region was small compared to the average signal intensity. The reference sample will have constant intensity throughout the MC series since the image acquisition parameters, and thereby the relaxation time weighting, are constant. For each data set, the wood/reference intensities were scaled such that the wood/reference intensity is 1.0 for the highest intensity (highest MC) image in the series.

The data from the three hardwoods in Fig. 4 follow approximately the same trend, but the pine sample exhibits anomalous behavior. We

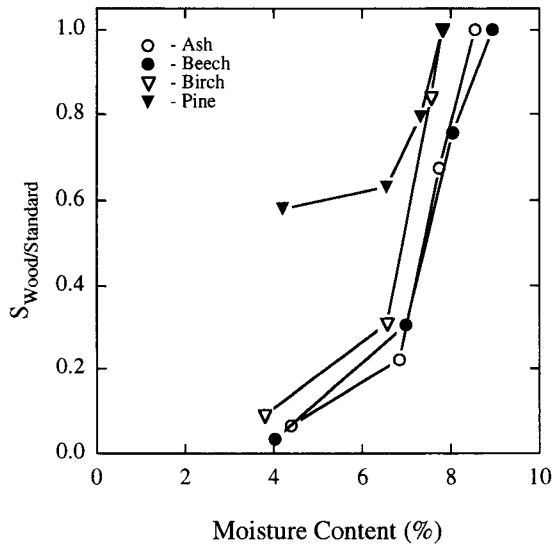


FIG. 4. Standardized signal intensities, $S_{\text{wood/reference}}$, from the spin-echo images of four wood species. The dependence of intensity on moisture content is strongly non-linear due to the effects of spin-spin relaxation. The anomalous behavior exhibited by the pine sample may be due to resins and other nonvolatile components. The lines between data points are drawn as a guide to the eye.

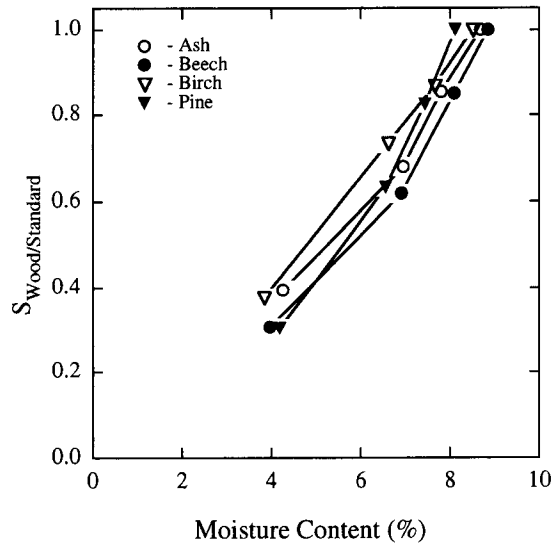


FIG. 5. Standardized signal intensities, $S_{\text{wood/reference}}$, from the SPRITE images of four wood species. Once again the pine sample, the only softwood, exhibits anomalous behavior, although less severely than in the spin-echo images. The SPRITE images are a much better measure of the residual moisture content. The lines between data points are drawn as a guide to the eye.

believe this is due to resins in the wood that do not evaporate under the conditions of these experiments. The MR signals from these resins, with an anticipated long T_2 , will contribute significantly to the overall detected signal at low MC. At the lowest MC, there is a sharp break in the wood/reference intensity for all three hardwoods.

If the relaxation times were independent of MC, we would expect the plots of Fig. 4 to be linear. That this is not the case in the plot from the spin-echo images indicates that T_2 is shorter at lower MC, as previously discussed. The results from the SPRITE images, (Fig. 5) are much closer to being linear, indicating that the images are better maps of water content. Note also that the intercept of the SPRITE images is much closer to zero, indicating once more that these images are a better measurement of the true water content. One would not anticipate an ideal intercept at the origin for Fig. 5 due to the likelihood of detecting some residual ^1H signal from hydrogen containing

structures in the wood, other than water. The vast majority of the MR signal from rigid ^1H containing structures in the wood (fiber itself) will decay to zero in 30 to 50 μsec (Araujo et al. 1992) and thus these structures will exhibit near zero, but perhaps not absolutely zero, intensity in an image.

For the spin-echo images, image intensity decreases by a factor of approximately 20 from the highest to lowest moisture content (Fig. 4). The water content, however, decreases by only a factor of 2. Over the same hydration range, intensity from the SPRITE images (Fig. 5) decreases by a factor of 3. Once more this indicates significant attenuation of the experimental signal, beyond simple water loss, due to spin-spin relaxation (Eq. [1]). In low water content wood materials, the SPRITE method is clearly the more effective imaging technique. It has the added benefit that we now have the ability to acquire images from very low moisture content wood materials. The fact that the SPRITE image inten-

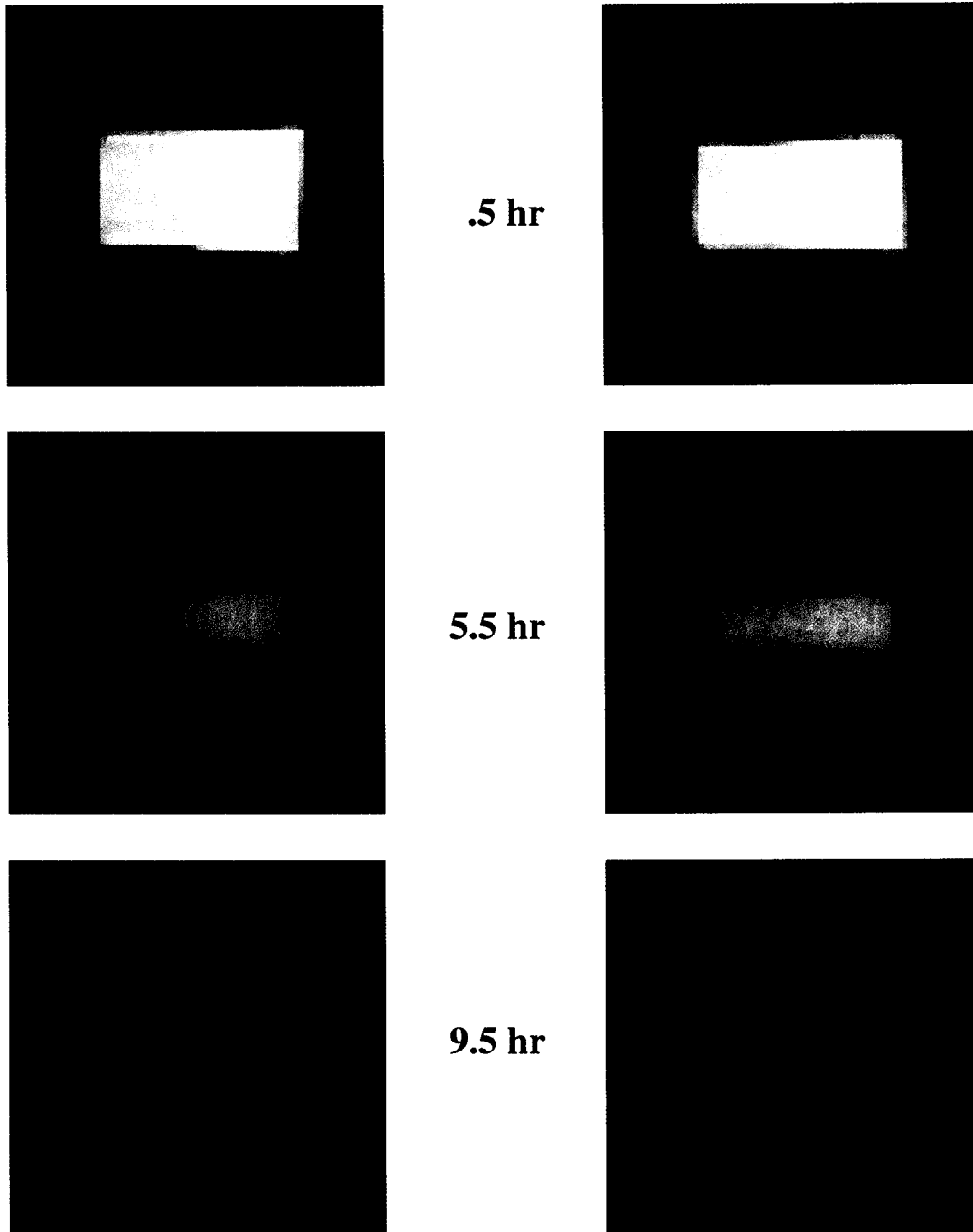


FIG. 6. Spin-echo and SPRITE images, of a white ash sample, acquired during active drying at 0.5, 5.5, and 9.5 hours after the onset of drying. The image field of view is 8 cm \times 8 cm. As expected, moisture loss is more rapid in the longitudinal direction (the shorter dimension). Drying is asymmetric in the other direction due to the morphology of the sample.

sities decrease by a factor of 3, when the moisture content decreases by a factor of 2, shows that even the SPRITE images, with these measurement parameters, are not a linear measure of water content. We anticipate that SPRITE images with a variable encoding time, t_p , could be fit to Eq. (3) and the true moisture content ρ_0 , readily determined, thus producing a more linear measure. These improvements, and others intended to increase the experimental sensitivity, are in progress.

As outlined above, short t_p SPRITE images are essentially moisture content maps. This makes SPRITE an ideal tool for the quantification of moisture concentration and, over time, moisture migration. Two-dimensional spin-echo and SPRITE images, averaged over the radial dimension, of residual water content in a white ash sample undergoing forced drying are presented in Fig. 6. Images were acquired every 45 min. for 23 h. The displayed images correspond to 0.5, 5.5, and 9.5 h after the onset of drying. As before, high quality images may be acquired with the SPRITE method at much lower moisture contents than are possible with the spin-echo method. The SPRITE images are maps of water concentration during drying, which in future studies should allow quantitative analyses of drying and fluid impregnation processes in wood materials.

CONCLUSIONS

We have demonstrated that a new MRI imaging sequence, SPRITE, is a dramatic improvement over conventional spin-echo methods for the visualization of low moisture content woods. The SPRITE images are higher quality, and the method greatly reduces the lower limit of moisture content that may be successfully studied. SPRITE images may be proton density (moisture content) weighted, thus the technique has potential for quantifying, potentially in real time, fluid concentration and fluid displacement in wood materials.

Extractives in pine, and presumably other softwoods, confuse the interpretation of spin-

echo MRI images, where the signal intensity is weighted by the spin-spin relaxation times of the various components. SPRITE images are weighted by proton density, making analytical interpretation more straightforward.

ACKNOWLEDGMENTS

Professors Balcom and Schneider thank NSERC of Canada for equipment and operating grants in addition to a Steacie memorial fellowship (2000–2002) awarded to Balcom. The MRI Centre is supported through an NSERC Major Facilities Access award.

REFERENCES

- ARAUJO, C. D., A. L. MACKAY, J. R. T. HAILEY, K. P. WHITTALL, AND H. LE. 1992. Proton magnetic resonance techniques for characterization of water in wood: Application to white spruce. *Wood Sci. Technol.* 26(2): 101–113.
- AXELSON, D. E., A. KANTZAS, AND T. EADS. 1995. Single point ^1H magnetic resonance imaging of rigid solids. *Can. J. Appl. Spec.* 40(1):16–26.
- BALCOM, B. J. 1998. SPRITE Imaging of short relaxation time nuclei. *In* P. Bluemler, B. Blümich, R. Botto, E. Fukushima, eds. *Spatially resolved magnetic resonance: Methods, materials, medicine, biology, rheology, geology, ecology, hardware*. Wiley/VCH, Weinheim, Germany.
- , R. P. MACGREGOR, S. D. BEYEA, D. P. GREEN, R. L. ARMSTRONG, AND T. W. BREMNER. 1996. Single-point ramped imaging with T_1 enhancement. *J. Mag. Res. A* 123:131–134.
- BEYEA, S. D., B. J. BALCOM, P. J. PRADO, A. R. CROSS, C. B. KENNEDY, R. L. ARMSTRONG, AND T. W. BREMNER. 1998. Relaxation time mapping of short T_2^* nuclei with single-point imaging (SPI) methods. *J. Mag. Res.* 135: 156–164.
- BLÜMICH, B. 2000. *NMR imaging of materials*. Clarendon Press, Oxford, UK. pp. 199–243.
- CALLAGHAN, P. T., 1991. *Principles of nuclear magnetic resonance microscopy*. Clarendon Press, Oxford, UK, pp. 121–128.
- CHANG, S. J., J. R. OLSON, AND P. C. WANG. 1989. NMR imaging of internal features in wood. *Forest Prod. J.* 39(6):43–49.
- COATES, E. R., S. J. CHANG, AND T. W. LIAO. 1998. A quick defect detection algorithm for magnetic resonance images of hardwood logs. *Forest Prod. J.* 48(10):68–74.
- CRC HANDBOOK OF CHEMISTRY AND PHYSICS. 2000. CRC Press, Cleveland, OH.
- FILBOTTE, S., R. S. MENON, A. L. MACKAY, AND J. R. T. HAILEY. 1990. Proton magnetic resonance of western red cedar. *Wood Fiber Sci.* 22(4):362–376.

- GRAVINA, S., AND D. G. CORY. 1994. Sensitivity and resolution of constant time imaging. *J. Mag. Res. B* 104(1):53-61.
- HALL, L. D., AND V. RAJANAYAGAM. 1986. Evaluation of the distribution of water in wood by use of three dimensional proton NMR volume imaging. *Wood Sci. Technol.* 20:329-333.
- , ———, W. A. STEWART, AND P. R. STEINER. 1986a. Magnetic resonance imaging of wood. *Can. J. For. Res.* 16:423-426.
- , ———, ———, AND S. CHOW. 1986b. Detection of hidden morphology of wood by magnetic resonance imaging. *Can. J. For. Res.* 16:684-687.
- KENNEDY, C. B., I. V. MASTIKHIN, AND B. J. BALCOM. 1998. MRI of polymeric materials using single point ramped imaging with T_1 enhancement (SPRITE). *Can. J. Chem.* 76:1753-1765.
- KLAFTER, J., AND J. M. DRAKE, EDs. 1989. *Molecular dynamics in restricted geometries*. Wiley, New York NY, PP. 1-22.
- MACGREGOR, R. P., H. PEEMOELLER, M. H. SCHNEIDER, AND A. R. SHARP. 1983. Anisotropic diffusion in wood. *J. Appl. Poly. Sci., Appl. Poly. Symp.* 37:901-909.
- MACMILLAN, B. 1996. An NMR investigation of the dynamical characteristics of water absorbed in Nafion. Ph.D. thesis, University of New Brunswick, Fredericton, NB.
- MEDER, R., R. A. FRANICH, AND P. T. CALLAGHAN. 1999. ^{11}B magnetic resonance imaging and MAS spectroscopy of trimethylborate-treated radiata pine wood. *Solid State Nuclear Mag. Res.* 15:69-72.
- MENON, R. S., A. L. MACKAY, S. FILBOTTE, AND J. R. HAILEY. 1989. Quantitative separation of NMR images of water in wood on the basis of T_2 . *J. Mag. Res.* 82: 205-210.
- PEARCE, R. B., B. J. FISHER, T. A. CARPENTER, AND L. D. HALL. 1997a. Immobilized long-lived free radicals at the host-pathogen interface in sycamore (*Acer pseudoplatanus L.*). *New Phytol.* 135:675-688.
- , P. P. EDWARDS, T. L. GREEN, P. A. ANDERSON, B. J. FISHER, T. A. CARPENTER, AND L. D. HALL. 1997b. Water distribution in fungal lesions in the wood of sycamore, *Acer pseudoplatanus*, determined gravimetrically and using nuclear magnetic resonance imaging. *Physiol. Molecular Plant Pathol.* 50:371-390.
- PEEMOELLER, H., M. E. HALE, M. H. SCHNEIDER, A. R. SHARP, AND D. W. KYDON. 1985. Study of restricted diffusion in wood. *Wood Fiber Sci.* 17(1):110-116.
- PRADO, P. J., B. J. BALCOM, I. V. MASTIKHIN, C. B. KENNEDY, R. L. ARMSTRONG, AND A. LOGAN. 1999. Magnetic resonance imaging of gases. A SPRITE Study. *J. Mag. Res.* 137:324-332.
- QUICK, J. J., J. R. T. HAILEY, AND A. L. MACKAY. 1990. Radial moisture profiles of cedar sapwood during drying: A proton magnetic resonance study. *Wood Fiber Sci.* 22(4):404-412.
- RIGGIN, M. T., A. R. SHARP, R. KAISER, AND M. SCHNEIDER. 1979. Transverse NMR relaxation of water in wood. *J. Appl. Poly. Sci.* 23:3147-3154.
- SKAAR, C. 1988. *Wood-water relations*. Springer-Verlag, NY, New York, PP. 178-206.
- TROUTMAN, M. Y., I. V. MASTIKHIN, B. J. BALCOM, T. M. EADS, AND G. R. ZIEGLER. 2001. Moisture migration in soft-panned confections during engrossing and aging as observed by magnetic resonance imaging. *J. Food Eng.* 48:257-267.
- WAANA, C. M. 1994. A study of molecular dynamics in water-cellulose systems using NMR. Ph.D. thesis, University of New Brunswick, Fredericton, NB.
- WANG, P. C., AND S. J. CHANG. 1986. Nuclear magnetic resonance imaging of wood. *Wood Fiber Sci.* 18(2): 308-314.